Transdermal skin patch based on reduced graphene oxide: A new approach for photothermal triggered permeation of ondansetron across porcine skin

Florina Teodorescu, Gurvan Queniat, Catherine Foulon, Marie Lecoeur, Alexandre Barras, Samia Boulahneche, Mohmaed Salah Medjram, Thomas Hubert, Amar Abderrahmani, Rabah Boukherroub, et al.

Post-print

Transdermal skin patch based on reduced graphene oxide: A new approach for photothermal triggered permeation of ondansetron across porcine skin

Authors: Florina Teodorescu[a], Gurvan Quéniat[ab], Catherine Foulon[c], Marie Lecoeur[c], Alexandre Barras[a], Samia Boulahneche[ad], Mohmaed Salah Medjram[d], Thomas Hubert[e], Amar Abderrahmani[b], Rabah Boukherroub[a], SabineSzunerits[a]

a Univ. Lille, CNRS, Centrale Lille, ISEN, Univ. Valenciennes, UMR 8520 - IEMN, F-59000 Lille, France
b University Lille, CNRS, CHU Lille, Institut Pasteur de Lille, European Genomic Institute of Diabetes (EGID) FR 3508, UMR 8199, Génomique Intégrative et Modélisation des Maladies Métaboliques, F-59000 Lille, France
c Univ. Lille, EA 7365 - GRITA-Groupe de Recherche sur les formes Injectables et les Technologies Associées, F-59000 Lille, France
d Laboratoire de Génie Chimique et Environnement de Skikda (LGCES), Université 20 Août 1955-Skikda, Algeria
e University Lille 2, CHU Lille, INSERM, European Genomic Institute of Diabetes (EGID), INSERM, UMR 1190, F-59000 Lille, France

First published: 30/11/2016
DOI: 10.1016/j.jconrel.2016.11.029

Abstract.

The development of a skin-mounted patch capable of controlled transcutaneous delivery of therapeutics through thermal activation provides a unique solution for the controlled release of active principles over long-term periods. Here, we report on a flexible transdermal patch for photothermal triggered release of ondansetron (ODS), a commonly used drug for the treatment of chemotherapy-induced nausea and vomiting and used as model compound here. To achieve this, a dispersion of ODS-loaded reduced graphene oxide (rGO-ODS) nanosheets were deposited onto Kapton to produce a flexible polyimide-based patch. It is demonstrated that ODS loaded Kapton/rGO patches have a high drug delivery performance upon irradiation with a continuous laser beam at 980 nm for 10 min due to an induced photothermal heating effect. The ability of ODS impregnated Kapton/rGO patches as transdermal delivery scaffolds for ODS across the skin is in addition investigated using porcine ear skin as a model. We show that the cumulative quantity and flux of ODS passing the skin are highly depending on the laser power density used. At 5 W cm^{-2} irradiation, the ODS flux across pig skin was determined to be 1.6 µg cm^{-2} h^{-1} comparable to other approaches. The use of tween 20 as skin enhancer could significantly increase the ODS flux to 13.2 µg cm^{-2} h^{-1}. While the skin penetration enhancement is comparable to that obtained using other well-known permeation enhancers, the actual superiority and interest of the proposed approach is that the Kapton/rGO photoactivatable skin patch can be loaded with any drugs and therapeutics of interest, making the approach extremely versatile. The on demand delivery of drugs upon local laser irradiation and the

DOI: https://doi.org/10.1016/j.jconrel.2016.11.029 – Journal: Journal of Controlled Release – Post-print

possibility to reload the interface with the drug makes this new drug administration route very appealing.

Graphical abstract

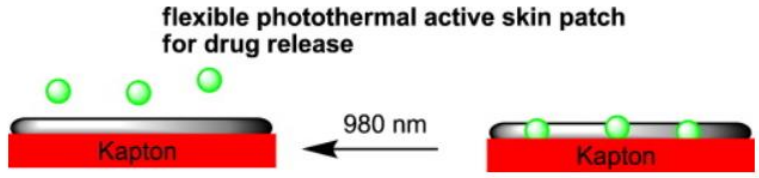

1. Introduction

Recent achievements in materials science and nanotechnology have led to the development of various suited materials as carriers of drugs and therapeutics [1–9]. Particularly, graphene-based materials have gained a great deal of interest in this domain due to their high loading capacity [3,10–16]. For example, the loading ratio (weight ratio of loaded drug to carrier) of graphene oxide (GO) towards doxorubicin hydrochloride, an anticancer drug, could reach up to 200%, much higher than that of other nanocarriers such as nanoparticles with a loading ratio lower than 100% [13].

Various external stimuli have been employed to initiate drug release from graphene-based matrices, including pH [13,14,17], electrical [18], electrochemical [10,11,19] and light [15,20]. For on-demand release of drugs with high spatial and temporal resolution, light stimulation has shown to be an effective approach. Such photo-controlled drug delivery systems are often based on light induced photoreactions, which trigger drug release from the nanocarriers [6,21,22]. In the case of graphene-based drug-loaded scaffolds, near-infrared (NIR) light triggered photothermal effects are above all used to drive the release of therapeutics [15,20,23]. The effectiveness of graphene as NIR-absorbing photothermal agent compared to other carbon allotropes is enhanced by the rapid light-to-heat conversion of reduced graphene oxide (rGO) under low-power NIR irradiation [24]. The readily manufacturing of NIR laser pointer devices and the transparency of tissue in the NIR region make such delivery approaches amendable to clinical settings [25]. Besides a recent report by Matteini et al., where photothermal films composed of dispersion of rGO nanosheets loaded with doxorubicin in chitosan scaffolds have been proposed as delivery systems [20], photoablation of tumors by cellular uptake of graphene-based nanomatrices is most widely investigated [16,26]. However, photothermal active patches mounted on the skin, capable of controlled transcutaneous delivery of therapeutics through thermal activation, might provide a unique solution for the controlled release of active principles over long-term periods. It could thus represent a promising biomedical technology for the treatment of certain types of diseases such as cancer, diabetes and chronic pain.

In this work, the development of a drug loaded transdermal skin patch, where the embedded therapeutics can be released at demand using a photothermal trigger is presented (Fig. 1).

DOI: https://doi.org/10.1016/j.jconrel.2016.11.029 – Journal: Journal of Controlled Release – Post-print

Transdermal therapeutic systems, mostly known under the name of transdermal patches, are systems that deliver effective amount of drugs to the systemic circulation *via* the skin [27–30]. Compared to oral systems, they have the advantage of overcoming first-pass metabolism of drugs in the gut and liver, improved patient compliance and reduced side effects, and have proven to be of great therapeutic utility. However, there are several factors which make the transdermal delivery of various drugs a challenging issue. The unique structural features of the *stratum corneum*, the outermost layer of the skin, only permits lipophilic drugs with small molecular weight (< 500 Da) to penetrate *via* passive diffusion [31]. A variety of methods have been tested to enhance the permeability of the *stratum corneum*. The design of chemical formulations, with chemical skin enhancers such as solvents and surfactants, as well as the synthesis of co-drug modified therapeutics to disrupt the structure of the *stratum corneum*, have been proposed [32–34]. On the other hand, physical techniques including mechanical and thermal approaches have been investigated to generate micrometer disruptions in the *stratum corneum* structure. The use of microneedles filled with drugs is one of the painless strategies to pierce the *stratum corneum* and to enhance drug permeation [10,29,35]. Laser ablation-enhanced transdermal drug delivery using wavelengths of CO_2 and Er:YAG lasers at 10,600 nm and 2940 nm have been investigated to heat the skin to hundreds of degrees for a very short period of time in order to disrupt the *stratum corneum* structure [36,37]. Other studies have shown that heat can be used as an external trigger to increase skin permeability and is expected to enhance in addition blood vessel permeability, thus facilitating transdermal drug delivery [38,39]. Temperature dependent drug release through a hyperthermia effect is also one of the approaches used to trigger efficient drug release from graphene nanomatrices [15,20,23].

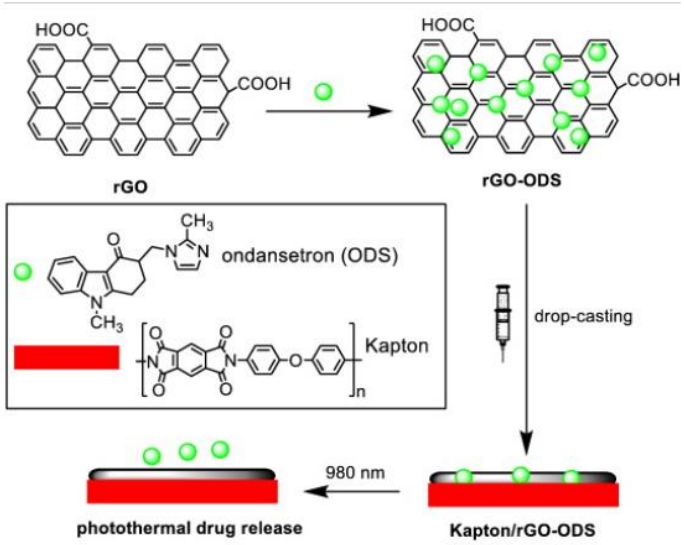

Figure 1.
Schematic illustration of the fabrication of a flexible photoactive skin-patch based on ODS-loaded rGO deposited onto Kapton.

We investigate, here, if a transdermal skin patch obtained by impregnation of rGO nanosheets with ondansetron (ODS) as a model drug and deposited onto a flexible polyimide-based interface, Kapton, can deliver therapeutics across the skin at demand using NIR photothermal triggering to initiate drug release from the patch (Fig. 1). NIR light causes little tissue absorption and minimal thermal effect, but can penetrate up to 10 cm into soft tissues [40]. ODS, a selective

DOI: https://doi.org/10.1016/j.jconrel.2016.11.029 – Journal: Journal of Controlled Release – Post-print

5-HT3 receptor antagonist used in the treatment of nausea and vomiting related to cancer chemotherapy [41] was chosen as model drug. ODS appears to be a well suited transdermal agent as it has a molecular weight of 293 Da, a logP value of 2.07, and a pK_A of about 7.4 [28,42]. As passive transdermal delivery of ODS is very low, skin enhancers are normally added to pharmaceutical ODS formulations to enable *in vitro* skin permeation [43–45]. The interest in ODS motivated us to use this drug for the loading of the developed transdermal skin patch and to investigate the efficacy for ODS delivery through the skin upon NIR irradiation of the patch. With a pKa of 7.6, thus being positively charged at *stratum corneum* pH (between 4.5 and 6.8), it is hoped furthermore that the interaction with negatively charged cell junctions in the *stratum corneum* will result in enhanced percutaneous penetration activity.

2. Experimental section

2.1 Materials

Hydrogen peroxide (H_2O_2), sulfuric acid (H_2SO_4), sodium hydroxide (NaOH), dimethylsulfoxide (DMSO), hydrazine hydrate, acetonitrile (CH_3CN) and Tween 20 were purchased from Sigma-Aldrich (Darmstadt, Germany) and used as received. Ondansetron (ODS) and graphene oxide (GO) were purchased from Biotrend (Zurich, Switzerland) and Graphenea (Spain), respectively. Kapton® HN Polyimide foils with a thickness of 125 μm were obtained from DuPont (Circleville, OH, USA).

2.2 Synthesis of reduced graphene oxide (rGO)

Graphene oxide (GO) was synthesized from graphite powder by a modified Hummers' method [46]. 5 mg of the synthesized GO were dispersed in 1 mL of water and exfoliated through ultrasonication for 3 h. This aqueous suspension of GO was used as a stock suspension in subsequent experiments. The reduction of GO to reduced graphene oxide (rGO) was performed by adding hydrazine hydrate (0.50 mL, 32.1 mM) to 5 mL GO aqueous suspension (0.5 mg mL^{-1}) in a round bottom flask and heated in an oil bath at 100 °C for 24 h. During this time, the reduced GO gradually precipitates out of the solution. The product was isolated by filtration over a polyvinylidene difluoride (PVDF) membrane with a 0.45 μm pore size, washed copiously with water (5 × 20 mL) and methanol (5 × 20 mL), and dried in an oven at 60 °C for 6 h [47].

2.3. Loading of rGO with ondansetron (ODS)

rGO (1–5 mg mL^{-1}) was sonicated with ondansetron (500 μg mL^{-1}) for 2 h under stirring. All samples were centrifugated at 13,500 rpm for 30 min. The concentration of ODS loaded onto the rGO matrix was determined using UV/Vis spectrometry (see Fig. 3A). A calibration curve (inset Fig. 3A) was established at 310 nm using a series of ODS solutions of different concentrations. The concentration of ODS remaining in the supernatant solution used for loading of rGO was first determined using the calibration curve. The ODS concentration in the patch was calculated according to equation

$$[ODS]_{rGO} = [ODS]_{initial} - [ODS]_{supernatent} \quad (1)$$

DOI: https://doi.org/10.1016/j.jconrel.2016.11.029 – Journal: Journal of Controlled Release – Post-print

with $[ODS]_{rGO}$ = concentration of ODS on the rGO matrix (μg mL^{-1})

with $[ODS]_{initial}$ = initial concentration of ODS in solution (500 μg mL^{-1})

with $[ODS]_{supernatent}$ = concentration of ODS in supernatant (μg mL^{-1})

2.4. Preparation of Kapton/rGO-ODS flexible skin patch

Kapton foils (10 × 10 mm^2) were cleaned with acetone in an ultrasonic water bath for 30 min, followed with isopropanol for 10 min and then dried under a nitrogen flow. The cleaned Kapton foils were modified with rGO-ODS by drop-casting (100 μL) three times, followed by drying at room temperature for several hours.

2.5. Characterization of the ondansetron loaded Kapton/rGO

2.5.1. Scanning electron microscopy (SEM)

SEM images were obtained using an electron microscope ULTRA 55 (Zeiss, France) equipped with a thermal field emission emitter and three different detectors (EsB detector with filter grid, high efficiency In-lens SE detector and Everhart-Thornley Secondary Electron Detector).

2.5.2. UV/Vis measurements

Absorption spectra were recorded using a Perkin Elmer Lambda UV/Vis 950 spectrophotometer in a 1-cm quartz cuvette. The wavelength range was 200–1100 nm.

2.5.3. Zeta potential measurements

The zeta potential was determined using dynamic light scattering principle (Malvern Zetasizer, NanoZS). The values of zeta potential of rGO (50 μg mL^{-1}) and their mixtures with ODS in water at various pH (4, 6, 7 and 9) were recorded.

2.5.4. Contact angle measurements

Water contact angles were measured using 2 μL of deionized water. A remote-computer controlled goniometer system (DIGIDROP by GBX, France) was used for measuring the contact angles. The accuracy is ± 1°. All measurements were performed in ambient atmosphere at room temperature.

2.6. HPLC/UV method for quantification of ondansetron permeation through skin

Chromatographic analyses were performed using a Waters system (Milfors, MA, USA) equipped with a gradient quaternary 600E metering pump, an online degasser apparatus, a 717 plus autosampler and a 996 photodiode array detector. Data were collected and processed on a computer running with Empower solftware (version 2) from Waters. Separations were carried out on a reversed-phase Kinetex C18 (100 × 4.60 mm *i.d.*, 2.6 μm) column (Phenomenex, Le Pecq, France) preceded by a guard C18 column (1 × 4.60 mm). Isocratic elution was performed

DOI: https://doi.org/10.1016/j.jconrel.2016.11.029 – Journal: Journal of Controlled Release – Post-print

at 1 mL min^{-1} with a mobile phase consisting of H_2O/acetonitrile (80/20 - v/v) mixture, containing 0.1% formic acid. The column was thermostated at 25 °C. Samples were filtered through a 0.45 μm regenerated cellulose membrane prior to loading the column (injection volume: 20 μL). Detection was performed at 310 nm. This method permits the analysis of ODS in < 6 min with a linear range between 0.1 and 100 μg L^{-1}, according to a linear regression ($R^2 > 0.999$).

2.7. Photothermal release of ODS into solution

Release experiments were performed into 1 mL deionized water. The skin patch was irradiated with a continuous mode laser (Gbox model, Fournier Medical Solution) with an output light at 980 nm at various power densities (1–10 W cm^{-2}) for various time intervals (1–60 min). Thermal images were captured by an Infrared Camera (Thermovision A40) and treated using ThermaCam Researcher Pro 2.9 software. The quantity of drug released was determined by assessment of ondansetron concentration in the supernatant after irradiation, by UV spectrometry method, at 310 nm, using a calibration curve with ODS concentration ranging from 1 to 100 μg mL^{-1}.

2.8. Skin permeation experiments

Skin permeation studies were performed using fresh porcine ear skin purchased in a local slaughterhouse. After thorough rinsing the pig ear with distilled water, the cartilage and the adipose tissue layer were removed with the aid of a surgical scalpel. The skin was gently shaved and cut into 1.8 cm^2 circular pieces. After measurement of its thickness using a digimatic micrometer (Mitutoyo, France), the skin was used immediately thereafter for diffusion experiments.

ODS skin diffusion experiments were carried out using static Franz diffusion cells (SES GmbH, Analyse System, Bechenheim, Germany) exhibiting an effective area of 0.64 cm^2. After filling the receptor compartment with degassed PBS (1 ×, pH 7.4), the solution was maintained at 32 °C and stirred with a magnetic stirring bar at around 500 rpm. The porcine skin was carefully clamped between the donor and the receptor compartment (3.1 mL). Pre-incubation in the receptor compartment medium for 1 h was performed before the ODS modified skin patch was applied to the skin previously wetted with 100 μL of water to insure contact between the patch and the skin. The diffusion experiment was started and followed for 6 h. The ODS modified skin patch was irradiated with a continuous wave laser at 980 nm for 10 min using different power densities (0–10 W cm^{-2}), just after the patch application. At determined time intervals (1 h), 250 μL aliquots of diffused solution were removed from the receptor compartment and analysed by HPLC. After each sampling, an equal volume of fresh diffusion medium was added to the receptor compartment to maintain a constant volume. All experiments were performed in triplicates.

The release and permeation profiles were determined by plotting the cumulative amount of ODS in the receptor compartment (Q_{exp}) (Eq. (2)) against time.

$$Q_{exp} = c_n \times V + \sum_{i=1}^{n-1} V_s \times c_i \quad (2)$$

DOI: https://doi.org/10.1016/j.jconrel.2016.11.029 – Journal: Journal of Controlled Release – Post-print

with Q_{exp} = cumulative amount of ODS diffused through the skin (μg)

c_n = concentration of ODS (μg mL^{-1}) determined at the n^{th} sampling interval

V = volume of the acceptor phase (receptor compartment) (mL)

The ODS flux (*J*) was determined according to Eq. (3):

$$J = A/S \quad (3)$$

with *J* = flux of ODS through the skin (μg cm^{-2} h^{-1})

A = linear slope of the cumulative amount *versus* time curves in equilibrium conditions (μg h^{-1})

S = surface of the membrane of the Franz cell (0.64 cm^2)

2.9. Effect of surfactant Tween 20 on skin permeation of ODS

The effect of Tween 20 on the permeation efficiency of ODS through pig skin was evaluated in two ways. In the first approach, Tween 20 was integrated into the rGO/ODS mixture by sonicating rGO (1 mg mL^{-1}) with ondansetron (500 μg mL^{-1}) and Tween 20 (500 μg mL^{-1}) for 2 h under stirring. The samples were centrifugated at 13.500 rpm for 30 min, washed with water and drop casted (100 μL, three times) onto cleaned Kapton foils, followed by drying at room temperature for several hours.

The other experimental set up consisted in applying the ODS modified skin patch to the skin previously wetted with 200 μL of a mixture of water/tween 20 (85/15 w:w %). The diffusion experiments were performed as explained in 2.8.

2.10. Evaluation of ODS trapped in the skin

To estimate the amount of ODS trapped in the skin, the skin was added into water/ice mixture for 10 min and sonicated in the presence of ZnO_2 beads (4 mm in diameter), before being centrifuged for 30 min at 13500 rpm using an ultracentrifuge (Mini Scan Fuge ORIGIO). The liquid phase was collected and filtrated through a 0.1 μm Nylon filter (Whatman Puradisc 13 mm) and the amount of ODS determined by HPLC/UV.

2.11. Skin staining and histology

Immediately after the laser release studies, the porcine skin was cleaned in water, dissected and placed in paraformaldehyde (4% v/v) for 24 h in order to fix the tissue. The samples were paraffined, sectioned and stained with the Masson's trichrome dye.

DOI: https://doi.org/10.1016/j.jconrel.2016.11.029 – Journal: Journal of Controlled Release – Post-print

3. Results and discussion

3.1. Design and characteristics of rGO/Kapton flexible photoactive skin patches

The fabrication of a flexible photoactive skin patch is based on drop-casting a suspension of drug-loaded rGO onto 1 cm2 large films of poly (4,4′-oxydiphenylene-pyromellitimide), registered under the name Kapton (Fig. 1).

The choice of Kapton as a patch material is based on some of its interesting physico-chemical properties. Highly aromatic polyimide resins such as Kapton have high thermal stability (> 300 °C), a high glass transition temperature (T_g > 200 °C), proven chemical resistance as well as excellent flexibility and adhesive properties [48–50]. The optical absorption of GO, rGO, rGO/Kapton is depicted in Fig. 2A. The absorbance intensity at 980 nm was found to be boosted in the Kapton film. The SEM image of a rGO/Kapton matrix (Fig. 2B) shows that the entire interface is coated with a thin film of wrinkling paper-like structures as expected for rGO. The rGO/Kapton patches are stable in air for several months.

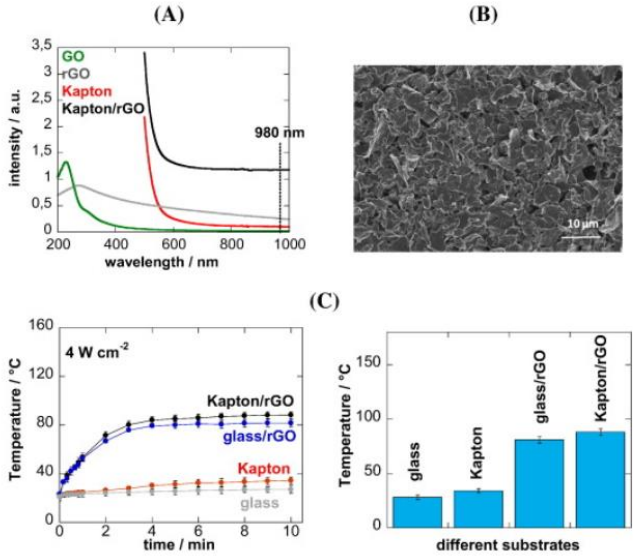

Figure 2.

(A) UV/Vis absorption spectra of an aqueous solution of GO (2 mg mL− 1, green), quartz interfaces coated with rGO thin films by drop-casting (2 mg mL− 1, three times, grey), Kapton film (red) and Kapton coated by drop casting with rGO (2 mg mL− 1, three times black) (2 mg mL− 1);
(B) SEM image of rGO loaded Kapton patch; (C) Comparison of photothermal heating capacity of glass (grey), Kapton (red), glass/rGO (blue) and Kapton/rGO (black) of water under NIR illumination (980 nm) for 10 min at 4 W cm− 2 together with final temperature in form of a bar diagram.

DOI: https://doi.org/10.1016/j.jconrel.2016.11.029 – Journal: Journal of Controlled Release – Post-print

3.2. Photothermal properties of the skin patch

As the aim of the work is the development of a skin patch that can be activated by a continuous-wave NIR to provide on-demand drug delivery over an extended period of time due to an induced temperature change, the photothermal heating ability of the patch was determined. The use of NIR light in the range of 700–1100 nm is necessary, as the absorption of NIR photons of the skin is minimal in this spectral region. The wavelength of 980 nm is widely used in the construction of biomedical lasers and thus was used throughout the work. While this wavelength falls within the vibration onset of water molecules with consequently higher absorption cross section, absorption by water molecules at 980 nm is not causing problems in most cases [51,52], and might be beneficial for the photothermal delivery across the skin. One of the main advantages using 980 nm excitation rather than 810 nm is associated with deeper tissue penetration and a low level degradation of biomolecules and cellular photo-damage. The photothermal heating ability of Kapton, and rGO/Kapton was determined under NIR irradiation (Fig. 2C). Even though Kapton has a strong absorption at 980 nm, it shows no photothermal heating ability even under high laser power irradiation of 4 W cm^{-2}. Upon coating with rGO, temperatures up to 88 °C are reached within 10 min. To evaluate if Kapton has any synergistic effect on the final temperature, the photothermal heating curves of glass and glass modified by drop casting with rGO are recorded (Fig. 2C). Glass alone does not heat as expected. The glass/rGO interface exhibits a somewhat smaller final solution temperature of 81 °C compared to the 88 °C achieved using rGO/Kapton, indicating a rather small impact of Kapton on the photothermal properties of the patch.

3.3. Loading of skin patch with ondansetron (ODS)

ODS was integrated into rGO by sonicating a suspension of rGO (1–5 mg mL^{-1}) in water (pH 7) with 500 μg mL^{-1} of ODS for 4 h. The loading mechanism is believed to occur through π-π stacking and/or charge interactions between rGO and the positively charged pyridine network of ODS, although other contributions such hydrogen bonding and/or van der Waals interactions cannot be excluded. The loading capacity of rGO for ODS was evaluated by measuring the concentration of ODS in solution before and after loading using UV/Vis spectrometric measurements at 310 nm. At this wavelength, ODS displays a well-defined absorption band which scales linearly with its concentration in solution (Fig. 3A). As can be seen from Fig. 3B, ODS loading increased upon increasing the ratio of [rGO]/[ODS]. A loading efficiency of 98% was reached for a rGO/ODS ratio of 4 (Fig. 3C). Further increase of the [rGO]/[ODS] ratio to 6 did not result in any increase of ODS loading at pH 7. The loading capacity of rGO was found to be pH dependent, with higher ODS loading at pH ≥ 7 (Fig. 3D). With a pKa of 7.6, under pH 7.6 ODS is mainly in a cationic form (99.97%, 97.5% and 80% at pH 4, 6 and 7, respectively) whereas at pH 9 it is mainly neutral (96.2%). As π-π stacking interactions are pH independent, the higher ODS loading under basic conditions might be due to a better solubility of ODS.

DOI: https://doi.org/10.1016/j.jconrel.2016.11.029 – Journal: Journal of Controlled Release – Post-print

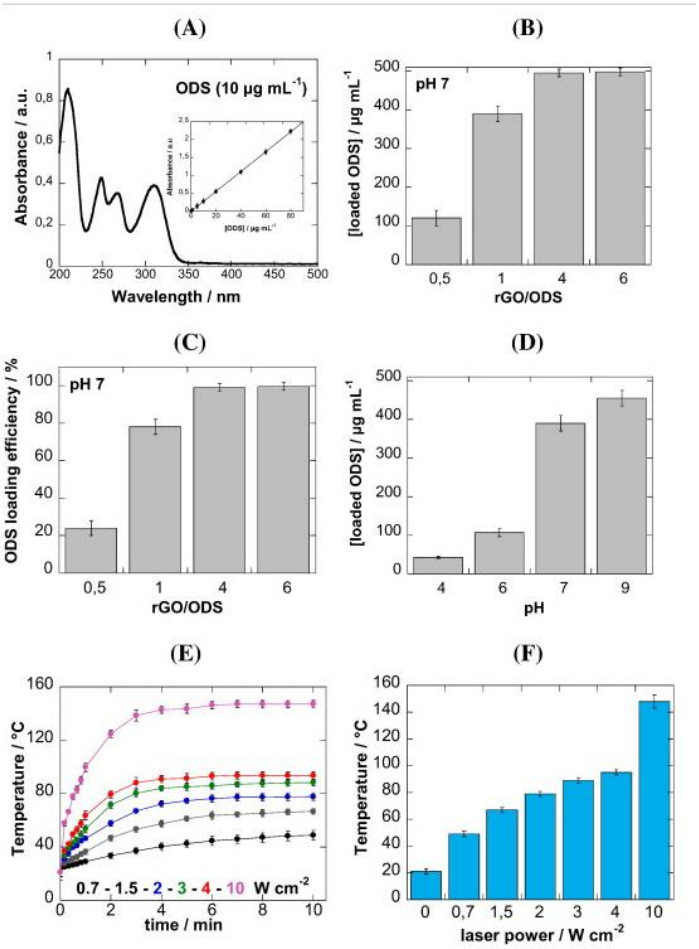

Figure 3

ODS loading on the skin patch:
(A) UV/Vis spectrum of ODS solution (inset: calibration curve;
(B) ODS (500 µg mL^{-1}) loading capacity of rGO as a function of rGO content at pH 7;
(C) ODS loading efficiency;
(D) Influence of pH on ODS loading (500 µg mL^{-1}) onto rGO (2 mg mL^{-1});
(E) Photothermal heating curves of water using a Kapton/rGO patch under NIR illumination (980 nm) at different laser power densities using a continuous wave laser;
(F) Change in water solution temperature (1 mL) during illumination of Kapton-rGO patch at 980 nm for 10 min as a function of laser power density.

The photothermal heating curves as a function of laser power of a patch formed by drop-casting a rGO-ODS (ratio of 4) onto Kapton are seen in Fig. 3E, F. The presence of ODS does not impact the solution temperature as the same temperatures were reached at 4 W cm^{-2} for Kapton/rGO-ODS (Fig. 3E) and Kapton/rGO (Fig. 2C). Depending on the laser power density used, the solution temperature can be tuned between 20 and 155 °C. This wide temperature range achieved allows investigation of the effect of temperature on skin disruption and on drug delivery. In the case of laser ablation-enhanced transdermal drug delivery, the skin gets heated

DOI: https://doi.org/10.1016/j.jconrel.2016.11.029 – Journal: Journal of Controlled Release – Post-print

to hundreds of degrees for very short time periods (μs-ms), which perforates or removes the *stratum corneum* (SC): temperatures between 100 and 150 °C results in disordering of the SC lipid structures; temperatures between 150 and 200 °C disrupt the SC keratin network structures, while temperatures above 300 °C result in a decomposition and vaporization of keratin to create micropores in the SC, which leads to increased skin permeability [53]. Pulsed CO_2 and Er:YAG lasers are required, because their emitting mid-infrared wavelength matches the absorption wavelength of water molecules, resulting in strong light absorption and skin heating [36,54]. NIR light alone, as used here, is however not sufficient to remove the *stratum corneum*.

3.4. Release of ondansetron (ODS) from ODS Kapton/rGO patches

Before determining the amount of ODS released during photothemal activation, the long term stability of the ODS loaded Kapton/rGO patch was established. Around 5 ± 2% of ODS desorbs from the patch after 1 day immersion in a solution of pH 7, indicating a stable interface over time. Fig. 4A displays the amount of photochemically released ODS upon illumination of the patch at 980 nm for 10 min with a continuous laser at different laser powers. The proportion of ODS released increases with increasing the laser power density. At 0.7 W cm^{-1}, only a small fraction of ODS was released. A temperature of 50 °C (Fig. 3F) seems not sufficient to change the affinity between ODS and rGO. At a laser power of 3 W cm^{-1}, corresponding to 89 °C, the ODS proportion released after 10 min reached a maximal value. Despite increasing the laser power density to 10 W cm^{-1} did not increase further ODS release (Fig. 4A). An important feature of the patch is its reusability. Reloading of ODS onto the patch after photothermal release could be performed with the same efficiency for at least 6 cycles (Fig. 4B), making the patch of particular interest for the development of on-demand delivery platforms. The ODS loaded patch also provides sustained drug release upon NIR trigger. Fig. 4C exhibits the total amount of ODS released from the patch over 9 days when activated once a day for 10 min by laser illumination at 980 nm (3 W cm^{-2}). While in the first day 15% (75 μg mL^{-1}), on the second day 14% (70 μg mL^{-1}) and the third day 10% (50 μg mL^{-1}) of ODS were released from the matrix, thereafter the amount is kept constant at 8.8% (44 μg mL^{-1}). This experiment demonstrates that the photoactivated Kapton/rGO interface facilitates the release of multiple drug doses at demand using the same patch, without being recharged. Under the chosen conditions the patch can be indeed used for a least a week safely.

DOI: https://doi.org/10.1016/j.jconrel.2016.11.029 – Journal: Journal of Controlled Release – Post-print

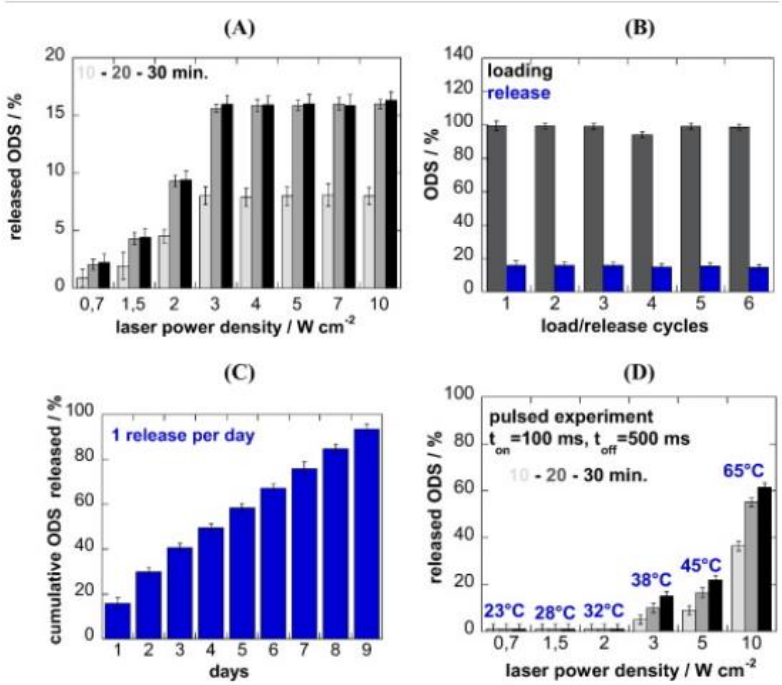

Figure 4.

ODS release:
(A) Concentration of photothermally released ODS into water (pH 7) from Kapton/rGO patch (formed by mixing 500 μg mL^{-1} ODS with 1 mg mL^{-1} rGO) using a continous wave laser at 980 nm, 0.7–10 W cm^{-2} with illumination time of 10 min;
(B) Reloading (at pH 7 with 500 μg mL^{-1}) and release of ODS (980 nm, 10 min, 3 W cm^{-2}) from patch for 6 cycles;
(C) Cumulative fractional release of ODS over 9 days upon activation once a day for 10 min (980 nm, 3 W cm^{-2}); (D) Concentration of photothermally released ODS into water (pH 7) from Kapton/rGO patch upon pulsed light irradiation at 980 nm and 3 W cm^{-2}.

It has been previously demonstrated that photo-thermal ablation using pulsed rather than continuous laser light produces instant heating, which ceases at the end of each light pulse, resulting in much less temperature increase in the skin and favorable release [55]. In addition, the release profile of ODS under laser pulses of 100 ms, with a dead time of 500 ms, has been examined (Fig. 4D). Under laser light pulses activation, only a fraction of ODS was released when compared to that under continuous illumination (Fig. 4A). As the temperatures obtained using pulsed illumination were much lower than those under continuous one, it seems that the temperature plays a major role in the release.

3.5. Transdermal ODS delivery through pig skin

To determine the impact of NIR laser irradiation on the skin penetration ability and profile of ODS from Kapton/rGO-ODS patch reservoir, the transdermal flux of ODS through skin was investigated using a Franz diffusion cells set-up. Skin permeation studies were performed using

DOI: https://doi.org/10.1016/j.jconrel.2016.11.029 – Journal: Journal of Controlled Release – Post-print

porcine ear skin since its *stratum corneum* is very similar to that of human *stratum corneum*[56]. The thickness of the skin was determined as being 1.6 ± 0.4 mm. As dry skin provides a significant barrier to drug diffusion, the pig skin was wetted before the deposition of the Kapton/rGO patch. The Kapton/rGO-ODS patch was irradiated for 10 min at 980 nm at different laser power densities between 0 and 10 W cm^{-2} and the passage of ODS through the skin was followed over 6 h and quantified using HPLC/UV (see SI Fig. S1) where a linear relationship between peak area and ODS concentration between 0.1 and 10 μg mL^{-1} is obtained, with a limit of detection of 0.1 μg mL^{-1}.

As can be seen from Fig. 5A, no passive transdermal diffusion of ODS was observed. This was validated both by depositing (1) ODS loaded Kapton/rGO patches onto the pig skin without laser stimulation or (2) when 200 μL of an ODS solution (100 μg mL^{-1}) were deposited on the skin. This is in line with reported data by others [43,44].

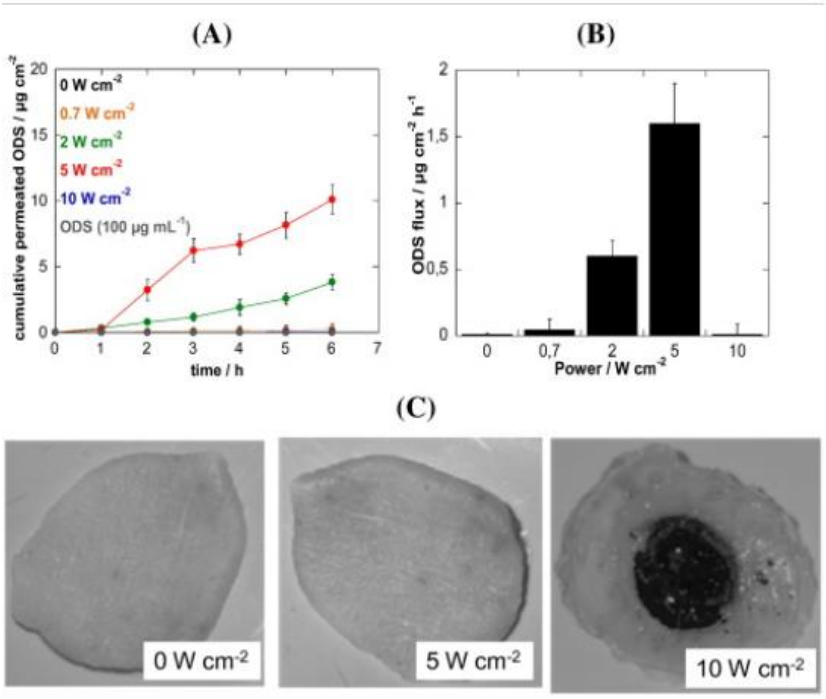

Figure 5

(A) *In vitro* permeation profiles of ODS (cumulative amount permeated *vs* time) through porcine skin from Kapton/rGO-ODS patches formed by mixing 500 μg mL^{-1} ODS with 1 mg mL^{-1} rGO upon light irradiation for 10 min using a continuous wave laser at 980 nm at different laser power densities; (0.7–10 W cm^{-2});
(B) Flux of ODS determined from panel A;
(CD) Photographs of pig skin before and after laser irradiation at 5 and 10 W cm^{-2} for 10 min.

In vitro release profiles of ODS upon laser irradiation indicate a laser power density correlated with increase in the quantity of ODS crossing the skin (Fig. 5A). After a lag time of about 1 h, transdermal ODS delivery is observed when laser power densities of 2 and 5 W cm^{-2} were

DOI: https://doi.org/10.1016/j.jconrel.2016.11.029 – Journal: Journal of Controlled Release – Post-print

used, with a more efficient penetration of ODS at the higher laser power density. While a constant increase of ODS permeation is seen in the case of 2 W cm^{-2}, in the case of 5 W cm^{-2} ODS penetration is more effective in the first 3 h, then stagnates with a reuptake at longer penetration times.

This enhancement is correlated to the temperature increase at the vicinity of the skin from 34 °C (0.7 W cm^{-2}) to 41 °C (2 W cm^{-2}) and finally 60 °C (5 W cm^{-2}). Indeed, controlled heat application can significantly enhance local skin perfusion and drug uptake from patches with correlate with an increased ODS transdermal delivery [57]. Surprisingly, application of a laser power density of 10 W cm^{-2}, which leads to even higher local temperature of ≈ 89 °C, shows no ODS passage over time. Such temperatures should result in a disorder of the lipid structures of the *stratum corneum* and probably in the disruption of the keratin network structures of *stratum corneum*, promoting drug penetration through the skin [36]. Different to laser ablation, in our case, the heat pulse is longer and heat propagation deeper into the tissue is expected, which might prevent ODS penetration, once damaged. Fig. 5C shows photographic images of the pig skin before and after laser irradiation at 5 and 10 W cm^{-2}. It can be noticed, that while no significant burns are seen until laser power densities of 5 W cm^{-2}, the pig skin was strongly burned at 10 W cm^{-2}.

The results of the laser irradiation of ODS Kapton/rGO patches using power densities of 5 W cm^{-2} were thus investigated in more details. To determine if the rest of the ODS, which has not passed the skin, is retained in the skin rather than passed through, the amount of skin trapped ODS left was determined. Indeed, from the 495 μg ODS initially loaded on the Kapton/rGO patch, after 6 h, 70 ± 10 μg was found to be trapped in the skin. In total, 79.6 μg ODS (16%) has thus has been released from the skin patch upon illumination at 5 W cm^{-2}, which is in accordance with results obtained in water (Fig. 4B).

From Fig. 5A, the ODS flux (J) across pig skin at 5 W cm^{-2} irradiation was determined to be J = 3.1 μg cm^{-2} h^{-1} for the first 3 h and then to decrease to J = 1.6 μg cm^{-2} h^{-1} thereafter (Fig. 5B). These values are comparable to that reported by Mashru et al. at pH 7.4 with an ODS flux of J = 2.52 μg cm^{-2} h^{-1} [58]. The results are also in line with the permeation parameters of ODS through exercised hairless mouse skin with a flux of J = 4.04 μg cm^{-2} h^{-1} reported by Gwak et al. using binary diethylene glycol monoethyl ether (DGME)/propylene glycol manocaprylate (PGMC) vehicles with a DGME/PGMC ratio of 1/100 [45].

Considering that the usual oral dose of ODS is between 16 and 32 mg a day and the oral bioavailability of ODS is 60%, for an effective transdermal delivery system, about 10–20 mg a day should be delivered *via* the skin into the blood circulation, *i.e.* 2.5–5 mg each 6 h [45]. Considering that a 25 cm^2 patch could be used, an ODS delivery of about 480 μg every 6 h can be reached, which would necessitate currently the use of several patches.

3.6. Histological analysis of laser-irradiated pig skin

The impact of the laser-irradiation on the skin structure was in addition taken into account by performing some histological investigations immediately after the laser activation experiments. Masson's trichrome dye was used for staining as it is commonly used in order to distinguish cells from a specific tissue from cells of other connective tissues by distinguishable colorations of each tissue. Using this dye, keratin and muscle fibers are colored red, collagen and bone blue

DOI: https://doi.org/10.1016/j.jconrel.2016.11.029 – Journal: Journal of Controlled Release – Post-print

or green, cytoplasm red or pink, and cell nuclei are brown to black. As can be seen in Fig. 6, no significant histological changes were observed up to a laser power density of 2 W cm^{-2}. In the case of 5 W cm^{-2}, which resulted in a large enhanced ODS permeation, modification of the skin epidermis structure is noticed. A total disruption of the *stratum corneum* is observed, which is in line with the possibility of transdermal ODS delivery. The collagen cell structure changes to a keratin like (scar tissue).

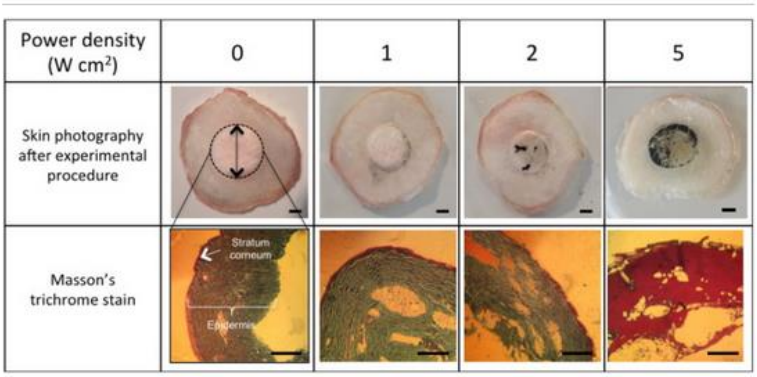

Figure 6

Representative photographes and histology of pig ear skin after treatment with different laser power densities at 980 nm for 10 min. Scale bar = 0.5 mm.; the black spots on the skin are due to rGO.

3.7. Effect of addition of penetration enhancer on the ODS flux

The addition of penetration enhancers to transdermal delivery systems is known to improve drug penetration through the skin either by altering the skin barrier or by modifying the thermodynamic activity of penetrates [32]. We opted for the use of surfactant Tween 20, a known efficient skin enhancer used for ODS transdermal delivery [44]. Fig. 7A shows the *in vitro* permeation profiles of ODS through porcine skin using either a skin patch where Tween 20 had been integrated into the rGO/ODs formulation and when the porcine skin was simply wetted with 200 μL of a solution of Tween 20 (15 wt.% in water) before the Kapton/rGO-ODS patch was placed onto the skin. Integration of Tween 20 into the skin patch (Kapton/rGO-ODS-tween 20) results in about 2.8 times higher permeated ODS, with an ODS flux of 4.49 μg cm^{-2} h^{-1}. However, the ODS flux was significantly enhanced to 13.2 ± 1.5 μg cm^{-2} h^{-1} when Tween 20 was directly deposited onto the pig skin and not integrated into the patch formulation. With a skin patch of 25 cm^2 about 2 ± 0.2 mg of ODS are delivered every 6 h, a therapeutically correct dose.

DOI: https://doi.org/10.1016/j.jconrel.2016.11.029 – Journal: Journal of Controlled Release – Post-print

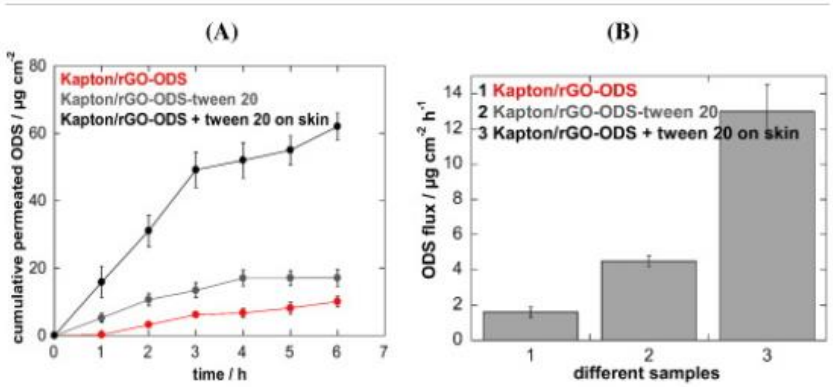

Figure 7

In vitro permeation profiles of cumulative permeated ODS through porcine skin upon light irradiation for 10 min using a continous wave laser at 980 nm at 5 W cm^{-2}) from Kapton/rGO-ODS (red; formed by mixing 500 µg mL^{-1} ODS with 1 mg mL^{-1} rGO), Kapton/rGO-ODS-tween 20 impregnated patches (grey; formed by mixing 500 µg mL^{-1} ODS with 500 µg mL^{-1} tween 20 and 1 mg mL^{-1} rGO) and from Kapton/rGO-ODS by wetting the skin with tween 20 (200 µL, 15 wt.% in water); (B) Flux of ODS determined.

4. Conclusion

In summary, we have developed a new strategy for the transdermal delivery of drugs using a composite patch based on Kapton modified with reduced graphene oxide (rGO). Ondansetron (ODS), a common drug to limit chemotherapy induced nausea and vomiting was used as a model drug to validate the concept. While ODS has a very good oral bioavailability, good water solubility and low molecular weight, its low permeability does not allow passive transdermal delivery. We could show that the use of ODS loaded Kapton/rGO patch upon laser-irradiation at 980 nm for 10 min results in an enhanced skin penetration without the use of permeation enhancers. The release strategy is based on a photothermally induced temperature increase, which modulates the affinity of ODS to rGO, and results in a controlled ODS release from the patch. Using porcine ear skin as a model the cumulative quantity of ODS passing the skin and the ODS flux are highly dependent on the laser power density used. At 5 W cm^{-2} irradiation, the ODS flux across pig skin was determined to be 1.6 µg cm^{-2} h^{-1}. The transdermal ODS dose delivered is smaller than the expected dose necessary for a therapeutic effect. However, the ODS flux could be increased to 13.2 µg cm^{-2} h^{-1} when Tween 20 was used for skin wetting. With a skin patch of 25 cm^2, a delivery of about 2 mg every 6 h [45] can thus be reached.

These results showing the potential of photothermal transdermal delivery using appropriate skin patches are encouraging and might open up new avenues for the development of NIR assisted transdermal delivery of different drugs using photothermal nanostructures. An intrinsic advantage for the proposed approach is that rGO is not delivered at the same time as the drug under consideration, minimizing regulatory issues as well as safety and toxicity issues. The fabrication costs of these skin patches are low as rGO can be produced on large scale industrially and as only small quantities of rGO (1 mg/mL) is needed for the fabrication of a patch. Furthermore, these patches can be easily recharged with ODS or any drug of interest by

DOI: https://doi.org/10.1016/j.jconrel.2016.11.029 – Journal: Journal of Controlled Release – Post-print

simple immersing Kapton/rGO into the respective solution. We believe that all these criteria make this photoactivable patch at demand an interesting alternative to other ODS formulations.

Acknowledgements

R.B. and S.S. gratefully acknowledge financial support from the Centre National de la Recherche Scientifique (CNRS), the Lille1 University, the CPER "Photonics for Society", and the Hauts-de-France Region. S.S thanks the Institut Universitaire de France (IUF) for financial support. Support from the European Union through H2020-MSCA-RISE-2015 (No. 690836, PANG) is also acknowledged.

References

1. M. Bikram, J.L. West **Thermo-responsive systems for controlled drug delivery**
   Expert Opin. Drug Deliv., 10 (2008), pp. 1077-1091
2. L. Deng, J. Ren, J. Li, J. Leng, Y. Qu, C. Lin, D. Shi **Magnetothermally responsive star-block copolymeric micelles for controlled drug delivery and enhanced thermo-chemotherapy**
   Nanoscale, 7 (2015), pp. 9655-9663
3. S. Goenka, V. Sant, S. Sant **Graphene-based nanomaterial for drug delivery and tissue engineering**
   J. Control. Release, 173 (2014), pp. 75-88
4. J.S. Im, B.C. Bai, Y.-S. Lee **The effect of carbon nanotubes on drug delivery in an electro-sensitive transdermal drug delivery system**
   Biomaterials, 31 (2010), pp. 1414-1419
5. D.A. La Van, T. McGuire, R. langer **Small-scale systems for in vivo drug delivery**
   Nat. Biotechnol., 21 (2003), p. 1184
6. S. Mura, J. Nicolas, P. Couvreur **Stimuli-responsive nanocarriers for drug delivery**
   Nat. Mater., 12 (2013), pp. 991-1003
7. D. Peer, J.M. Karp, S. Hong, O.C. Farokhzad, R. Margalit, R. Langer **Nanocarriers as an emerging platform for cancer therapy**
   Nat. Nanotechnol., 2 (2007), p. 751
8. C.L. Stevenson, J.T. Santini, R. Langer **Reservoir-based drug delivery systems using microtechnology**
   Adv. Drug Deliv. Rev., 64 (2012)
9. W. He, X. Guo, M. Zhang **Transdermal permeation enhancement of *N*-trimethyl chitosan for testosterone**
   Int. J. Pharm., 356 (2008), pp. 82-87
10. H. Lee, T.K. Choi, Y.B. Lee, H.R. Cho, R. Ghaffari, L. Wang, H.J. Choi, T.D. Chung, N. Lu, T. Hyeon, S.H. Choi, D.-H. Kim **A graphene-base electrochemical device with thermoresponsive microneedles for diabetes monitoring and therapy**
    Nat. Nanotechnol. (2016)
11. F. Teodorescu, L. Rolland, V. Ramarao, A. Abderrahmani, D. Mandler, R. Boukherroub, S. Szunerits **Electrochemically triggered release of human insulin from an insulin-impregnated reduced graphene oxide modified electrode**
    Chem. Commun., 51 (2015), pp. 14167-14170

DOI: https://doi.org/10.1016/j.jconrel.2016.11.029 – Journal: Journal of Controlled Release – Post-print

12. J. Hong, N.J. Shah, A.C. Drake, P.C. DeMurth, J.B. Lee, J. Chen, P.T. Hammond **Graphene multilayers as gates for multi-week sequential release of proteins from surfaces**
ACS Nano, 6 (2012), pp. 81-88
13. X. Yang, X. Zhang, Z. Liu, Y. Ma, Y. Huang, Y. Chen **High-efficiency loading and controlled release of doxorubicin hydrochloride on graphene oxide**
J. Phys. Chem. C, 112 (2008), pp. 17554-17558
14. K. Turcheniuk, A. Mororina, P. Subramanian, A. Barras, V. Zaitsev, V. Kuncser, A. Leca, A. Martoriati, K. Cailliau, J.-F. Bodart, R. Boukherroub, S. Szunerits **Insulin loaded iron magnetic nanoparticles-graphene oxide composites: synthesis, characterization and application for diabetes treatment**
RSC Adv., 4 (2014), pp. 865-875
15. H. Kim, W.J. Kim **Photothermally controlled gene delivery by reduced graphene oxide-polyethylenimine nanocomposite**
Small, 10 (2014), pp. 117-126
16. Z. Liu, J.T. Robinson, X. Sun, H. Dai **PEGylated nanographene oxide for delivery of water-insoluble cancer drugs**
J. Am. Chem. Soc., 130 (2008), pp. 10876-10877
17. L. Zhang, J. Xia, Q. Zhao, L. Liu, Z. Zhang **Functional graphene oxide as a nanocarrier for controlled loading and targeted delivery of mixed anticancer drugs**
Small, 6 (2010), pp. 537-544
18. C.L. Weaver, J.M. LaRosa, X. Luo, X.T. Cui **Electrically controlled drug delivery form graphene oxide nanocomposite films**
ACS Nano, 8 (2014), pp. 1834-1843
19. N.M. Kenna, P. Calvert, A. Morrin, G.G. Wallace, S.E. Moulton **Electro-stimulated release from a reduced graphene oxide composite hydrogel**
J. Mater. Chem. B, 3 (2015), p. 2530
20. P. Matteini, F. Tatini, L. Cavigili, S. Ottaviano, G. Ghini, R. Pini **Graphene as a photothermal switch for controlled drug release**
Nanoscale, 6 (2014), p. 7947
21. Z. Yan, D. zhao, X. Yi, R. Zhuo, F. Li **Steric protected and illumination-activated tumor targeting accessory for endowing drug-delivery system with tumor selectivity**
Adv. Funct. Mater., 24 (2014), pp. 1799-1807
22. D. Wang, S. Wu **Red-light responsive supramolecular valves for photocontrolled drug release from mesoporous nanoparticle**
Langmuir, 32 (2016), pp. 632-636
23. Y.-W. Wang, Y.-Y. Fu, Q. Peng, S.-S. Guo, G. Liu, J. Li, H.-H. Yang, G.-N. Chen **Dye-enhanced graphene oxide for photothermal therapy and photoacoustic imaging**
J. Mater. Chem. B, 1 (2013), pp. 5762-5767
24. Z.M. Markovic, L.M. Harhaji-Trajkovic, B.M. Todorovic-Markovic, D.P. Kepoc, K.M. Arsikin, S.P. Jovanovic, A.C. Pantovic, M.D. Dramicanina, V.S. Trajkovic **In vitro comparison of the photothermal anticancer activity of graphene nanoparticles and carbon nanotubes**
Biomaterials, 32 (2011), p. 1121
25. B.P. Timko, M. Arruebo, S.A. Shankrappa, J.B. McAlvin, O.S. Okonkwo, B. Mizrahi, C.F. Stefanescu, L. Gomez, J. Zhu, A. Zhu, J. Santamaria, R. Langer, D.S. Kohane **Near-infrared(actuated devices for remotely controlled drug delivery)**

DOI: https://doi.org/10.1016/j.jconrel.2016.11.029 – Journal: Journal of Controlled Release – Post-print

PNAS, 111 (2014), pp. 1349-1354
26. E. Akhavan, E. Ghaderi **Graphene nanomesh promises extremely efficient in vivo photothermal therapy**
Small, 9 (2013), p. 3593
27. T. Taqnner, R. Marks **Delivering drugs by the transdermal route: review and comments**
Skin Res. Technol., 14 (2008), pp. 249-260
28. G. Cevc, G. Blume, A. Schatzlein, D. Gebauer **The skin: a pathway for systematic treatment with patches and lipid-based carriers**
Adv. Drug Deliv. Rev., 18 (1996), pp. 349-378
29. D.P. Wermeling, S.L. Banks, D.A. Hudson, H.S. Gill, J. Gupta, M.R. Prausnitz, A.L. Stinchcomb **Microneedles permit transdermal delivery of a skin-impermeant medication to humans**
PNAS, 105 (2008), pp. 2058-2063
30. M.R. Prausnitz, S. Mittagotri, R. Langer **Current status and future potential of transdermal drug delivery**
Nat. Rev. Drug Discov., 3 (2004), pp. 115-124
31. T. Hampton **Breaking barriers in transdermal drug delivery**
J. Am. Med. Assoc., 293 (2005), p. 2083
32. A.C. Williams, B.W. Barry **Penetration enhancers**
Adv. Drug Deliv. Rev., 56 (2004), pp. 603-618
33. H.K. Vaddi, *et al.* **Human skin penetration of branched chain 3-O-alkyl ester and carbonate prodrugs of naltrexone**
Pharm. Res., 22 (2005), pp. 758-765
34. Y. Chen, Y. Shen, X. Gui, C. Zhang, W. Yang, M. Ma, S. Liu, M. Zhang, L.P. Wen **Transdermal protein delivery by coadminstered peptides identified via phage display**
Nat. Biotechnol., 24 (2006), pp. 455-460
35. S. Yang, F. Wu, J. Liu, G. Fan, W. Welsh, H. Zhu, T. Jin **Phase-transition microneedle patches for efficient and accurate transdermal delivery of insulin**
Adv. Mater., 25 (2015), pp. 4633-4641
36. Y. Li, L. Guo, W. Lu **Laser ablation-enhanced transdermal drug delivery**
Photon Lasers Med., 2 (2013), pp. 315-322
37. M.R. Prausnitz, R. Langer **Transdermal drug delivery**
Nat. Biotechnol., 26 (2008), pp. 1261-1268
38. J. Vanakoski, T. Seppala **Heat exposure and drugs. A review of the effects of hyperthermia and pharmacokinetics**
Clin. Pharmacokinet., 34 (1998), pp. 311-322
39. K.K. Peersen, M.L. Rousing, C. Jensen, L. Arendt-Nielsen, P. Gazerani **Effect of local controlled heat on transdermal delivery of nicotin**
Int. J. Physiol. Pathophysiol. Pharmacol., 3 (2011), pp. 236-242
40. B.P. Timko, D.S. Kohane **Prospects for near-infrared technology in remotely triggered drug delivery**
Expert Opin., 11 (2014), pp. 1681-1685
41. R. Patel, S. Naik, J. Patel, A. Baria **Formulation development and evaluation of mouth melting film of ondansetron**
Arch. Pharm. Sci. Res., 1 (2009), p. 212

DOI: https://doi.org/10.1016/j.jconrel.2016.11.029 – Journal: Journal of Controlled Release – Post-print

42. B. Godin, E. Touitou **Transdermal skin delivery: predictions for human from in vivo, ex vivo and animal models**
Adv. Drug Deliv. Rev., 59 (2007), pp. 1152-1161
43. A.S. Can, M.S. Erdal, S. Gungor, Y. Ozsoy **Optimization and characterisation of chitosan films for transdermal delivery of ondansetron**
Molecules, 18 (2013), pp. 5455-5471
44. R.M. Al Abood, S. Talegaonkar, M. Tariq, F.J. Ahmad **Microemulsion as a tool for the transdermal delivery of ondansetron for the treatment of chemotherapy induced nausea and vomiting**
Colloids Surf. B, 101 (2013), pp. 143-151
45. H.S. Gwak, I.S. Oh, I.K. Chun **Transdermal delivery of ondansetron hydrochloride: effects of vehicles and penetration enhancers**
Drug Dev. Ind. Pharm., 30 (2004), pp. 187-194
46. O. Fellahi, M.R. Das, Y. Coffinier, S. Szunerits, T. Hadjersi, M. Maamache, R. Boukherroub **Silicon nanowire arrays-induced graphene oxide reduction under UV irradiation**
Nanoscale, 3 (2011), pp. 4662-4669
47. S. Stankovich, D.A. Dikin, R.D. Piner, K.A. Kohlhaas, A. Kleinhammes, Y. Jia, Y. Wu, S.T. Nguyen, R.S. Ruoff **Synthesis of graphene-based nanosheets via chemical reduction of exfoliated graphite oxide**
Carbon, 45 (2007), p. 1558
48. P. A **Sensor Applications of Polyimides**
InTech (2012), pp. 199-214 (Chapter 10)
49. D. Wilson, H.D. Stenzenberger, P.M. Hergenrother **Polyimides**
Chapman & Hall, London (1990)
50. D. Sui, Y. Huang, L. Hung, J. Liang, Y. Ma, Y. Chen **Flexible and transparent electrothermal film heaters based on graphene materials**
Small, 7 (2011), pp. 3186-3192
51. Y.M. Bae, Y.I. Park, S.H. Nam, J.H. Kim, K. Lee, H.M. Kim, B. Yoo, J.S. Choi, K.T. Lee, T. Hyeon, Y.D. Suh **Endocytosis, intracellular transport, and exocytosis of lanthanide-doped upconverting nanoparticles in single living cells**
Biomaterials, 33 (2012), pp. 9080-9086
52. S.H. Nam, Y.M. Bae, B.J. Park, J.H. kim, H.M. Kim, J.S. Choi, K.T. Lee, T. Hyeon, Y.D. Suh **Long-term real-time tracking of lanthanide ion doped upconverting nanoparticles in living cells**
Angew. Chem. Int. Ed., 50 (2011), pp. 6093-6097
53. W.R. Lee, S.C. Shen, K.H. Wang, C.H. Hu, J.Y. Fang **The effect of laser treatment on skin to enhance an control transdermal delivery of 5-fluorouracil**
J. Pharm. Sci., 91 (2002), pp. 1613-1626
54. R. Kaufmann, C. Beier **Laser skin ablation: an update on aesthetic and medical indications**
Med. Laser Appl, 19 (2004), pp. 212-222
55. S. Ramadan, L. Guo, Y. Li, B. Yan, W. Lu **Hollow copper sulfide nanoparticle-mediated transdermal drug delivery**
Small, 8 (2012), pp. 3143-3150
56. K. Guth, M. Schäfer-Korting, E. Fabian, R. Landsiedel, B. van Ravenzwaay **Suitability of skin integrity tests for dermal absorption studies in vitro**
Toxicology, 29 (2015), pp. 113-123

DOI: https://doi.org/10.1016/j.jconrel.2016.11.029 – Journal: Journal of Controlled Release – Post-print

57. K.K. Petersen, M.L. Rousing, C. Jensen, L. Arendt-Niemsen, P. Gazerani **Effect of local controlled heat on transdermal delivery of nicotin**
Int. J. Physciol. Pathophysiol. Pharmacol., 3 (2011), pp. 236-242
58. R.C. Mashru, V.B. Sutariya, M.G. Sankalia, J.M. Sankalia
Effect on pH on in vitro permeation of ondansetron hydrochloride across porcine buccal mucosa
Pharm. Dev. Technol., 10 (2005), pp. 241-247

DOI: https://doi.org/10.1016/j.jconrel.2016.11.029 – Journal: Journal of Controlled Release – Post-print